Trajectory tracking for autonomous underwater vehicle: An adaptive approach

Jesus Guerrero, Jorge Torres, Vincent Creuze, Ahmed Chemori

Autonomous Underwater Vehicle Trajectory Tracking: An adaptive approach

J. Guerrero[a,], J. Torres[a], V. Creuze[b], A. Chemori[b]

[a] *Automatic Control Department, CINVESTAV, Mexico CDMX, Mexico*
[b] *LIRMM, CNRS-Universit Montpellier 2, Montpellier, France*

Abstract

During sea missions, underwater vehicles are exposed to changes in the parameters of the system and subject to persistent external disturbances due to the ocean current influence. These issues make the design of a robust controller a quite challenging task. This paper focuses on the design of a adaptive high order sliding mode control for trajectory tracking on an underwater vehicle. The main feature of the developed control law is that it preserves the advantages of robust control, it does not need the knowledge of the upper bound of the disturbance and easy tuning in real applications. Using Lyapunov concept, asymptotic stability of the closed-loop tracking system is ensured. The effectiveness and robustness of the proposed controller for trajectory tracking in depth and yaw dynamics are demonstrated through real-time experiments.

Keywords: Adaptive control, Underwater Vehicles, Sliding Mode Control, Real-Time Experiments

1. Introduction

Although the oceans cover 70% of the Earth's surface, almost the 95 % of the ocean remains unexplored according to data from the National Oceanic and Atmospheric Administration. Recently, underwater robotics has positioned itself as one of the essential areas within maritime exploration due to a long list of advantages as operational efficiency, mobility, and low operational cost [1].

Email address: `jguerrero@ctrl.cinvestav.mx` (J. Guerrero)

There are two main classes of underwater vehicles: The Remotely Operated Vehicles (ROVs), which require human piloting and the Autonomous Underwater Vehicles (AUVs), that refer to the submarines able to perform some tasks with full autonomy. A controller provides this autonomy required to position the vehicle at a specific point or to track a path. However, the design of the controller for an AUV is very challenging due to the nonlinearity, time-variance, random external disturbances, such as the environmental force generated by the sea's current fluctuation, and the difficulty in accurately modeling the hydrodynamic effect [2]. For these reasons, in recent years, different control techniques have been introduced for AUVs.

The Proportional-Derivative (PD) [3], the PD plus gravity and buoyancy compensation (PD+) [4, 5] and the Proportional Integral Derivative (PID) schemes are the most used techniques to control the position and orientation of commercial AUVs due to their design simplicity and their good performance. However, these controllers have some drawbacks. In one hand, the PD+ controller requires the exact knowledge of the gravitational and buoyancy force of the robot. On the other hand, it is well-known that the PID control performance is degraded when the plant is highly nonlinear, time-varying, or with significant time delays. Moreover, the listed controllers considering strong restrictive assumptions to simplify the mathematical description, resulting in an impractical controller due to its low robustness against disturbances. For this reason, many researchers concentrated their interests on the applications of robust control for underwater vehicles.

A broad class of robust controllers has been proposed for the trajectory tracking problem on AUV. For example, Fuzzy Logic Controllers (FLC) [6] [7], Neural-Network based control (NNC) [8, 9], Predictive control [10], Adaptive control [11], Sliding Modes Control (SMC) [12], High Order Sliding Modes Control (HOSMC) [13, 14] and so on. Each methodology has strengths and weaknesses. For instance, FLC has a simple structure, easy and cost-effective design. However, the controller tuning process might be a bit difficult because there is no stability criterion or FLC cannot be implemented for unknown systems.

The main advantage of NNC is their ability to learn from examples instead of requiring an algorithmic development from the designer. Nevertheless, NNC usually needs a long and computationally expensive training time which is not acceptable in many applications.

Adaptive control covers a set of techniques which provide a systematic approach for automatic adjustment of controllers in real time, in order to achieve or to maintain the desired level of system performance when the parameters of the dynamic model are unknown or change in time [15].

Sliding Mode Control (SMC) is another robust technique sometimes used in underwater vehicle control. This technique provides finite time convergence and robustness against bounded external disturbances. In its basic implementations, this controller can have aggressive control input behavior due to signum function which causes the undesirable chattering effect. However, there exist several ways to decrease the chattering effect, like replacing the signum function by a hyperbolic tangent, sigmoid or saturation functions [4] which smooths the control signal, but at the cost of loss of robustness because it constrains the sliding systems trajectories to the sliding surface's vicinity [16]. High Order Sliding Mode Control (HOSMC) is another conventional technique to reduce the chattering amplitude. This methodology takes advantage of quasi-continuous control which allows driving to the origin the sliding surface and its derivative in the presence of external disturbances. Finally, SMC with auto-adjustable [17] or dynamical gains [18] is an alternative solution to minimize the impact of the first order SMC drawbacks. In these techniques, an adaptive law is proposed to adjust the feedback controller gains according to the disturbance impact. There are many works following this philosophy. For instance, an adaptive first-order SMC for the set-point stabilization of an AUV is proposed in [19]. In this work, the control signal was divided into three terms: first, the equivalent control term to neglect the known parameters of the system. Second, the discontinuous signum function which minimizes the disturbance impact. Finally, the adaptive part which allows adjusting the feedback controller gains without the prior knowledge of the disturbance's bounds. In [20] an adaptive SMC for the trajectory tracking of pitch and yaw dynamics is proposed. In the design of the controller, it is taken into account the actuator's non-symmetric dead-zones and unknown disturbances. The adaptive law and the disturbance observer were designed to adjust the controller's gains while an anti-windup compensator was introduced to prevent actuator's saturation. Simulation and experimental results demonstrate the effectiveness of the proposed methodology. Also, an adaptive SMC for depth trajectory tracking of a ROV taking into account thruster's saturation and dead-zones is proposed in [21]. A three-layer feedforward neural network was used to identify unknown model parameters and adaptive laws to estimate the algorithm gains. Simulation results validate the correct behavior of the proposed method.

An adaptive second-order SMC for depth and yaw path following is proposed in [22]. A nonlinear function was introduced into the sliding surface to modify the damping ratio of the controller output. Then, the gain of the controller is estimated through the adaptive law which needs the disturbance's upper bound information. The efficiency of the proposed controller is demonstrated through real-time experiments. In [23], a multi-variable output feedback adaptive nonsingular terminal SMC for the four degrees of freedom trajectory tracking of AUV was developed. In this work, an adaptive observer with equivalent output injection was designed in order to estimate the system's states in finite time while the adaption control law stabilize the trajectory tracking error to a small field in finite time. Through computer simulations, the effectiveness of proposed controller was highlighted compared against similar methodologies. Also, in [24], an adaptive second-order fast nonsingular terminal SMC for AUV is proposed. In this work, the prior information about the upper bound of the disturbance is not required. Based on simulation results, chattering reduction and fast convergence is demonstrated when parameter uncertainties of 20 % and time variant disturbances were considered. In [25], an adaptive integral SMC for AUV stabilization was proposed. In this paper, two scenarios were considered. In the first case, it is assumed that the full system parameters were not available. In the second one, it is supposed that the system is affected by external disturbances. In both cases, the proposed adaptive law adjust the feedback controller gains in order to suppress the chattering effect.

In this context, the adaptive version of the well-known Super-Twisting (STW) controller is proposed in [18]. The STW algorithm was introduced initially in [26] ensures robustness with respect to parametric uncertainties and external disturbances while reducing the chattering effect. However, the main drawback of this method is that is necessary the knowledge of the boundaries of the disturbance gradients. In the mentioned adaptive version, the algorithm does not require any information on the bounds of the disturbance and its gradient. The method was developed for a single-input uncertain nonlinear system. Based on real-time experiments, the authors prove the good performance of the adaptive algorithm on the position control of an electro-pneumatic actuator.

In this paper, based on the previous results of [27] and [18], an adaptive high order sliding mode control for trajectory tracking of an AUV is developed. In this case, taking into account the procedure shown in the cited papers, the adaption law is applied to the Generalized Super-Twisting Algorithm (GSTA) which compared to the STW, the GSTA includes a linear

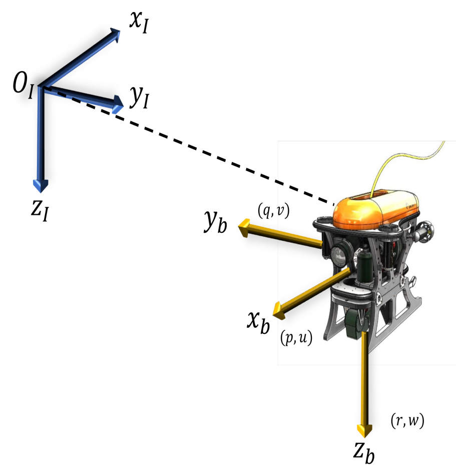

Figure 1: Underwater vehicle with the inertial-fixed frame (O_I, x_I, y_I, z_I) and the body-fixed frame (O_b, x_b, y_b, z_b).

version of the algorithm, the standard STA, and a STA with extra linear correction terms, that provide more robustness and convergence velocity [28]. The GSTA as well the STW, requires the knowledge of the bounds of the disturbance gradient. However, applying the adaptive law relaxes this condition, and the algorithm does not require it. Lyapunov arguments prove the stability of the proposed controller. Real-time experiments in depth and yaw trajectory tracking for an underwater vehicle demonstrate the effectiveness of the proposed method.

The remainder of this paper is organized as follows: The underwater vehicle dynamics equation is derived in Section 2. In Section 3, an adaptive high order sliding mode controller for trajectory tracking and its stability analysis is presented. In order to demonstrate the effectiveness of the proposed control scheme, real-time experiments for yaw and depth trajectory tracking tests for several scenarios are presented in Section 5. Finally, we make a brief conclusion on the paper in Section 6.

2. Dynamic Model

The dynamic model of underwater vehicles has been described in several works (see for instance ([4, 29, 30, 31, 32])).

The dynamics of an underwater vehicle involves two frames of reference: the body-fixed frame and the earth-fixed frame (see Fig. 1). Considering the generalized inertial forces, the hydrodynamic effects, the gravity and buoyancy contributions as well as the forces of the actuators (i.e., thrusters), the dynamic model of an underwater vehicle in matrix form, using the SNAME notation [33] and the representation introduced by [4], can be written as follows:

$$\begin{aligned} M\dot{\nu} + C(\nu)\nu + D(\nu)\nu + g(\eta) &= \tau + w_e(t) \\ \dot{\eta} &= J(\eta)\nu \end{aligned} \tag{1}$$

Where $\nu = [u, v, w, p, q, r]^T$ is the state vector of velocity relative to the body-fixed frame and $\eta = [x, y, z, \phi, \theta, \psi]^T$ represents the vector of position and orientation relative to the earth-fixed frame. From equation (1), the matrix of spatial transformation between the inertial frame and the frame of the rigid body can be as $J(\eta) \in \mathbb{R}^{6\times6}$. $M \in \mathbb{R}^{6\times6}$ is the inertia matrix where the effects of mass are included, $C(\nu) \in \mathbb{R}^{6\times6}$ is the Coriolis-centripetal matrix, $D(\nu) \in \mathbb{R}^{6\times6}$ represents the hydrodynamic damping matrix, $g(\eta) \in \mathbb{R}^6$ is the vector of gravitational/buoyancy forces and moments. Finally, $\tau \in \mathbb{R}^6$ is the control vector acting on the underwater vehicle and $w_e(t) \in \mathbb{R}^6$ defines the vector of external disturbances.

The presented formulation of the AUV dynamics is expressed in the body-fixed frame and can be transformed to the earth-fixed frame by using the kinematic transformations of the state variables and the model parameters as follows:

$$\begin{aligned} M_\eta(\eta) &= J^{-T}(\eta) M J^{-1}(\eta) \\ C_\eta(\nu, \eta) &= J^{-T}(\eta) \left[C(\nu) - M J^{-1}(\eta) \dot{J}(\eta) \right] J^{-1}(\eta) \\ D_\eta(\nu, \eta) &= J^{-T}(\eta) D(\nu) J^{-1}(\eta) \\ g_\eta(\eta) &= J^{-T}(\eta) g(\eta) \\ \tau_\eta(\eta) &= J^{-T}(\eta) \tau \\ w_\eta(t) &= J^{-T}(\eta) w_e(t) \end{aligned}$$

Based on these equalities, the dynamics (1) can therefore be rewritten in the earth-fixed frame as:

$$\underbrace{M_\eta(\eta)\ddot{\eta} + C_\eta(\nu, \eta)\dot{\eta} + D_\eta(\nu, \eta)\dot{\eta} + g_\eta(\eta)}_{f(\nu,\eta)} = \tau_\eta(\eta) + w_\eta(t) \tag{2}$$

Hydrodynamic loads dominate the AUV dynamics, and it is difficult to accurately measure or estimate the hydrodynamic coefficients that are valid for all vehicle operating conditions. As such, the system dynamics are not exactly known. Therefore, the system dynamics $f(\eta,\nu)$ given in (2) can be written as the sum of estimated dynamics $\hat{f}(\eta,\nu)$ and the unknown dynamics $\tilde{f}(\eta,\nu)$ as follows:

$$f(\eta,\nu) \quad = \quad \hat{f}(\eta,\nu) + \tilde{f}(\eta,\nu) \tag{3}$$

where:

$$\hat{f}(\eta,\nu) = \hat{M}_\eta(\eta)\ddot{\eta} + \hat{C}_\eta(\nu,\eta)\dot{\eta} + \hat{D}_\eta(\nu,\eta)\dot{\eta} + \hat{g}_\eta(\eta) \tag{4}$$
$$\tilde{f}(\eta,\nu) = \tilde{M}_\eta(\eta)\ddot{\eta} + \tilde{C}_\eta(\nu,\eta)\dot{\eta} + \tilde{D}_\eta(\nu,\eta)\dot{\eta} + \tilde{g}_\eta(\eta) \tag{5}$$

Moreover, the matrices of the unknown dynamics vector $\tilde{f}(\eta,\nu)$ are defined as $\tilde{M}_\eta = M_\eta - \hat{M}_\eta$, $\tilde{C}_\eta = C_\eta - \hat{C}_\eta$, $\tilde{D}_\eta = D_\eta - \hat{D}_\eta$ and $\tilde{g}_\eta = g_\eta - \hat{g}_\eta$.

Rewriting the system (2) into the estimated and unknown dynamics given by (3), we have:

$$\hat{M}_\eta(\eta)\ddot{\eta} + \hat{C}_\eta(\nu,\eta)\dot{\eta} + \hat{D}_\eta(\nu,\eta)\dot{\eta} + \hat{g}_\eta(\eta) = \tau_\eta(\eta) + \overline{w}(t) \tag{6}$$

where $\overline{w}(t) = w_\eta(t) - \tilde{f}(\eta,\nu)$.

Finally, note that the dynamical model of the AUV given by (6) only depends on the estimated values of system parameters shown in Equation (2).

3. Controller Design

In this section, the design of an adaptive gain high order sliding mode control for the AUV is addressed. The controller is based on the Generalized Super-Twisting Algorithm (GSTA) developed by [28] which is a general form of the original Super-Twisting Algorithm (STA) introduced by [26]. Inspired by the methodology presented in [27] where the authors developed an adaptive control law based on the original STW control for a single-input uncertain nonlinear system. In this work, we use the GSTA instead of the STA, and we extend the procedure shown in the cited article to a MIMO non-linear system such as the mathematical model of the AUV. Finally, the stability of the proposed controller is proven through Lyapunov function arguments.

3.1. Adaptive GSTA Design

First,let the next state variables:

$$\chi_1 = \eta \quad ; \quad \chi_2 = \dot{\eta}$$

Rewriting the model (6) as follows:

$$\begin{aligned} \dot{\chi}_1 &= \chi_2 \\ \dot{\chi}_2 &= F(\chi) + G(\chi)\tau_\eta + w(t) \end{aligned} \tag{7}$$

where:

$$\begin{aligned} F(\chi) &= -\hat{M}_\eta(\eta)^{-1}\left[\hat{C}_\eta(\nu,\eta)\dot{\eta} + \hat{D}_\eta(\nu,\eta)\dot{\eta} + \hat{g}_\eta(\eta)\right] \\ G(x) &= \hat{M}_n(\eta)^{-1}J^{-T}(\eta) \\ w(t) &= \hat{M}_\eta(\eta)^{-1}\overline{w}(t) \end{aligned}$$

Before introduce the design of the adaptive controller, it is necessary to consider the following assumptions:

Assumption 1. *The pitch angle is smaller than $\pi/2$, i.e., $|\theta| < \pi/2$.*

Assumption 2. *The perturbation $w(t)$ is a Lipschitz continuous signal.*

According to A1, the inverse of rotational matrix $J(\eta)$ exists. Then, $G(\chi)$ is not singular, therefore, its inverse exists.

According to A2, the time derivative of the external disturbance term $w(t)$ is bounded by

$$|\dot{w}_i(t,x)| \le L_i|\phi_2(\sigma)| \quad , \quad i = \overline{1,6}. \tag{8}$$

with $L_i \ge 0$ is a finite boundary but is not known.

From (7) it is possible to propose a sliding surface depending on the error that force the sliding mode in the manifold as follows:

$$\sigma = \dot{e}(t) + \Lambda \cdot e(t) \tag{9}$$

where $\sigma(t) := [\sigma_1, \sigma_2, \cdots, \sigma_6]^T$, $e(t) = \chi_1^d(t) - \chi_1(t)$ is the error vector an the desired trajectory is defined as $\chi_1^d(t) = [x_d(t), y_d(t), z_d(t), \phi_d(t), \theta_d(t), \psi_d(t)]^T$. $\dot{e}(t) = \chi_2^d(t) - \chi_2(t) = \dot{\chi}_1^d(t) - \dot{\chi}_1(t)$ is the time derivative of the error and $\Lambda =$

$diag(\Lambda_1, \Lambda_2, \cdots, \Lambda_6) \in \mathbb{R}^{6\times 6}$ is a diagonal positive definite matrix. Finally, the control law for the underwater vehicle is given as follows:

$$\tau_\eta = J^T \hat{M}_\eta(\eta)\big[\ddot{\chi}_1^d(t) + \Lambda\dot{e}(t) - F(\chi) - \upsilon\big] \tag{10}$$

where υ is the GSTA and is defined by:

$$\begin{aligned} \upsilon &= -K_1(t)\Phi_1(\sigma) + \lambda \\ \dot{\lambda} &= -K_2(t)\Phi_2(\tau) \end{aligned} \tag{11}$$

with the vectors $\Phi_1(\sigma) = [\phi_{11}, \phi_{12}, \cdots, \phi_{16}]^T$ and $\phi_2(\sigma) = [\phi_{21}, \phi_{22}, \cdots, \phi_{26}]^T$ and each element is given by:

$$\begin{aligned} \phi_{1i}(\sigma_i) &= \mu_{1i}|\sigma_i|^{1/2} sgn(\sigma_i) + \mu_{2i}\sigma_i \\ \phi_{2i}(\sigma_i) &= \frac{1}{2}\mu_{1i}^2 sgn(\sigma_i) + \frac{3}{2}\mu_{1i}\mu_{2i}|\sigma_i|^{1/2} sgn(\sigma_i) + \mu_{2i}^2\sigma_i \end{aligned}$$

where $\mu_{1i}, \mu_{2i} \geq 0$ with $i = \overline{1,6}$. $K_1(t) = diag(k_{11}(t), k_{12}(t), \cdots, k_{16}(t))$ and $K_2(t) = diag(k_{21}(t), k_{22}(t), \cdots, k_{26}(t))$ are the gain matrices which satisfy $K_1(t) = K_1(t)^T > 0$ and $K_2(t) = K_2(t)^T > 0$.

Moreover, if each element of the controller gain matrices is selected as follows:

$$\dot{k}_{1i}(t) = \begin{cases} \omega_i\sqrt{\frac{\varsigma_i}{2}} & \text{if } \sigma \neq 0 \\ 0 & \text{if } \sigma = 0 \end{cases} \tag{12}$$

$$k_{2i}(t) = 2\epsilon_i k_{1i}(t) + \beta_i + 4\epsilon_i^2 \tag{13}$$

where ω_i, ς_i, β_i and ϵ_i are arbitrary positive constants with $i = \overline{1,6}$. Then, for any initial condition $\sigma_i(0)$, the sliding surface $\sigma_i = 0$ will be reached in finite time.

3.2. Stability Analysis

Theorem 1. *From the underwater vehicle model* (2)*, suppose that the disturbance term $w(t)$ satisfies* (8)*. Then for any initial conditions $\chi(0)$, $\sigma(0)$ the sliding surface $\sigma = 0$ will be reached in finite time via AGSTA* (11) *with the adaptive gains selected as shown in equations* (12)*.*

Proof 1. *Taking into account the underwater vehicle model given by* (7)*, the the control law (10) and the sliding surface dynamics (9), leads to the following closed-loop error dynamics:*

$$\dot{\sigma} = -K_1(t)\Phi_1(\sigma) - K_2(t)\int_0^t \Phi_2(\sigma(\tau))d\tau + w(t) \tag{14}$$

Now, taking the following change of variables:

$$\begin{aligned} s_{1i} &= \sigma_i \\ s_{2i} &= -k_{2i}\int_0^t \phi_{2i}(\sigma_i(\tau))d\tau + w_i(t) \end{aligned}$$

Then (14) can be rewritten in scalar form ($i = \overline{1,6}$) as:

$$\begin{aligned} \dot{s}_{1i} =& -k_{1i}\Big[\mu_{1i}|s_{1i}|^{\frac{1}{2}}sgn(s_{1i}) + \mu_{2i}s_{1i}\Big] + s_{2i} \\ \dot{s}_{2i} =& -k_{2i}\Big[\frac{1}{2}\mu_{1i}^2 sgn(s_{1i}) + \frac{3}{2}\mu_{1i}\mu_{2i}|s_{1i}|^{\frac{1}{2}}sgn(s_{1i}) + \mu_{2i}^2 s_{1i}\Big] + \frac{d}{dt}w_i(t,\chi) \end{aligned}$$

Without loss of generality, we can represent the system with simplified notation:

$$\begin{aligned} \dot{s}_1 =& -k_1\Big[\mu_1|s_1|^{\frac{1}{2}}sgn(s_1) + \mu_2 s_1\Big] + s_2 \\ \dot{s}_2 =& -k_2\Big[\frac{1}{2}\mu_1^2 sgn(s_1) + \frac{3}{2}\mu_1\mu_2|s_1|^{\frac{1}{2}}sgn(s_1) + \mu_2^2 s_1\Big] + \frac{d}{dt}w(t,\chi) \end{aligned} \tag{15}$$

Then, the candidate Lyapunov Function is defined as:

$$V(s_1, s_2, k_1, k_2) = V_0(\cdot) + \frac{1}{2\varsigma_1}(k_1 - k_1^*)^2 + \frac{1}{2\varsigma_2}(k_2 - k_2^*)^2 \tag{16}$$

where ς_1,ς_2,k_1^*,k_2^* are positive constants and $V_0(\cdot)$ is given by:

$$V_0(s_1, s_2, k_1, k_2) = \xi^T P \xi \tag{17}$$

with:

$$\xi^T = [\phi_1(s_1), s_2] \tag{18}$$

and

$$P = P^T = \begin{bmatrix} \beta + 4\epsilon^2 & -2\epsilon \\ -2\epsilon & 1 \end{bmatrix} > 0 \tag{19}$$

Since β and ϵ are defined as an arbitrary positive constants, then P is a positive definite matrix. Moreover, note that the function $V_0(\cdot)$ satisfies the next form:

$$\lambda_{min}(P)\|\xi\|_2^2 \leq V_0(s,k) \leq \lambda_{max}(P)\|\xi\|_2^2 \tag{20}$$

where $\lambda_{min}(P)$ and $\lambda_{max}(P)$ are the smallest and greatest eigenvalue of P, respectively. $\|\xi\|_2^2 = |s_1| + 2|s_1|^{\frac{3}{2}} + s_1^2 + s_2^2$ is the Euclidean norm of ξ and the next inequality is satisfied as well:

$$|\phi(s_1)| \leq \|\xi\|_2 \leq \frac{V^{\frac{1}{2}}(\xi)}{\lambda_{\min}^{\frac{1}{2}}(P)} \tag{21}$$

Finally, it is important to note that the proposed candidate Lyapunov function $V(s_1, s_2, k_1, k_2)$ is a continuous, positive definite and differentiable function.

The procedure to find the time derivative of the function $V(\cdot)$ is divided into two main steps. First, the time derivative of $V_0(\cdot)$ is found. Second, the total time derivative of $V(\cdot)$ is shown.

***Step 1**. Noting that $\phi_2(s_1) = \phi_1'(s_1)\phi_1(s_1)$, the derivative of $V_0(\cdot)$ is obtained as:*

$$\begin{aligned}
\dot{V}_0 &= 2\xi^T P\dot{\xi} && (22)\\
&= 2\xi^T P \begin{bmatrix} \phi_1'\Big[-k_1\phi_1(s_1) + s_2\Big] \\ -k_2\phi_2(s_1) + \frac{d}{dt}w(t,\chi) \end{bmatrix} && (23)\\
&= 2\xi^T P \begin{bmatrix} \phi_1'(s_1)\Big[-k_1\phi_1(s_1) + s_2\Big] \\ \phi_1'(s_1)\phi_1(s_1)\Big[-k_2 + L\Big] \end{bmatrix} && (24)\\
&= \phi_1'(s_1) 2\xi^T P \underbrace{\begin{bmatrix} -k_1 & s_2 \\ -(k_2 - L) & 0 \end{bmatrix}}_{A(t,\chi)} \xi && (25)\\
&= \phi_1'(s_1)\xi^T(A^T(t,\chi)P + PA(t,\chi))\xi && (26)\\
&= -\phi_1'(s_1)\xi^T Q(t,\chi)\xi && (27)
\end{aligned}$$

where

$$Q(t,\chi) = \begin{bmatrix} 2k_1(\beta + 4\epsilon^2) - 4\epsilon(k_2 - L) & \star \\ k_2 - L - 2\epsilon k_1 - \beta - 4\epsilon^2 & 2\epsilon \end{bmatrix} \tag{28}$$

Selecting the gain $k_2 = 2\epsilon k_1 + \beta + 4\epsilon^2$, we have the following:

$$Q - 2\epsilon I = \begin{bmatrix} 2k_1\beta - 4\epsilon(\beta + 4\epsilon^2 - L) - 2\epsilon & -L \\ -L & 2\epsilon \end{bmatrix} \tag{29}$$

The matrix Q will be positive definite with a minimal eigenvalue $\lambda_{\min}(Q) \geq 2\epsilon$ if

$$k_1 > \delta_0 + \frac{\alpha_2^2}{4\epsilon\beta} + \frac{\epsilon\Big[2(\beta + 4\epsilon^2 + L) + 1\Big]}{2\beta} \tag{30}$$

Then, the time derivative of $V_0(\cdot)$ can be rewritten as:

$$\dot{V}_0 = -\phi_1'(s_1)\xi^T Q(t,x)\xi \leq -2\epsilon\phi_1'(s_1)\xi^T\xi = -2\epsilon\left(\mu_1\frac{1}{2|s_1|^{\frac{1}{2}}} + \mu_2\right)\xi^T\xi \tag{31}$$

Finally, using (21), the time derivative of $V_0(\cdot)$ is expressed as:

$$\dot{V}_0 \leq -\frac{\epsilon\lambda_{\min}^{\frac{1}{2}}(P)}{\lambda_{\max}(P)}\mu_1 V_0^{\frac{1}{2}}(s,k) - \frac{2\epsilon}{\lambda_{\max}(P)}\mu_2 V(s,k) \tag{32}$$

$$\leq -\gamma V_0^{\frac{1}{2}}(s,k) \tag{33}$$

with $\gamma = \mu_1\frac{\epsilon\lambda_{\min}^{\frac{1}{2}}(P)}{\lambda_{\max}(P)}$.

Step 2. *The time derivate of the Lyapunov function (16) is given by:*

$$\dot{V} = \dot{V}_0(\cdot) + \frac{1}{\varsigma_1}(k_1 - k_1^*)\dot{k}_1 + \frac{1}{\varsigma_2}(k_2 - k_2^*)\dot{k}_2 \tag{34}$$

$$\leq -\gamma V_0^{\frac{1}{2}}(s,k) + \frac{1}{\varsigma_1}(k_1 - k_1^*)\dot{k}_1 + \frac{1}{\varsigma_2}(k_2 - k_2^*)\dot{k}_2 \tag{35}$$

$$= -\gamma V_0^{\frac{1}{2}}(s,k) - \frac{\omega_1}{\sqrt{2\varsigma_1}}|k_1 - k_1^*| - \frac{\omega_2}{\sqrt{2\varsigma_2}}|k_2 - k_2^*| + \frac{1}{\varsigma_1}(k_1 - k_1^*)\dot{k}_1 + \tag{36}$$

$$+ \frac{1}{\varsigma_2}(k_2 - k_2^*)\dot{k}_2 + \frac{\omega_1}{\sqrt{2\varsigma_1}}|k_1 - k_1^*| + \frac{\omega_2}{\sqrt{2\varsigma_2}}|k_2 - k_2^*| \tag{37}$$

Using the Cauchy-Schwarz inequality, the first three terms of $\dot{V}$ can be synthesized as follows:

$$-\gamma V_0^{\frac{1}{2}}(s,k) - \frac{\omega_1}{\sqrt{2\varsigma_1}}|k_1 - k_1^*| - \frac{\omega_2}{\sqrt{2\varsigma_2}}|k_2 - k_2^*| \leq -\pi\sqrt{V(s,k_1,k_2)} \tag{38}$$

where $\pi = \min(\gamma, \omega_1, \omega_2)$.

Assuming that there exist positive constants k_1^* and k_2^* such that $k_1 - k_1^* < 0$ and $k_2 - k_2^* < 0$ are satisfied $\forall t \geq 0$. Then, the time derivative of V can be rewritten as:

$$\begin{aligned}\dot{V} &\leq -\pi\sqrt{V(s,k_1,k_2)} - |k_1 - k_1^*|\left(\frac{1}{\varsigma_1}\dot{k}_1 - \frac{\omega_1}{\sqrt{2\varsigma_1}}\right) - |k_2 - k_2^*|\left(\frac{1}{\varsigma_2}\dot{k}_2 - \frac{\omega_2}{\sqrt{2\varsigma_2}}\right) \\ &= -\pi\sqrt{V(s,k_1,k_2)} + \vartheta \end{aligned} \tag{39}$$

where:

$$\vartheta = -|k_1 - k_1^*|\left(\frac{1}{\varsigma_1}\dot{k}_1 - \frac{\omega_1}{\sqrt{2\varsigma_1}}\right) - |k_2 - k_2^*|\left(\frac{1}{\varsigma_2}\dot{k}_2 - \frac{\omega_2}{\sqrt{2\varsigma_2}}\right) \tag{40}$$

In order to preserve the finite time convergence it is necessary assure the condition $\vartheta = 0$ which will be achieved through the adaption gain laws as follows:

$$\dot{k}_1 = \omega_1\sqrt{\frac{\varsigma_1}{2}} \tag{41}$$

$$\dot{k}_2 = \omega_2\sqrt{\frac{\varsigma_2}{2}} \tag{42}$$

In brief, the adaptive gains k_1 and k_2 will be increase based on the dynamic and algebraic equations stated in (12) *until the condition* (30) *is reached. Then, the matrix Q will be positive definite and the finite time convergence will be assured according to* (39)*. Finally, when the sliding variable σ and its derivative converges to zero, the adaptive gains k_1 and k_2 will stop growing by making $\dot{k}_1 = 0$ as $\sigma = 0$. Subsequently, it is obtained the gain-adaptation law* (12)*.*

4. Real-Time Experimental Results

To demonstrate the practical feasibility of the developed controller, we applied the control algorithm to *Leonard* ROV (see Fig. 3), which is an underwater vehicle developed at the LIRMM (CNRS/University Montpellier, France). *Leonard* is a tethered underwater vehicle which is $75 \times 55 \times 45$ cm in dimension and 28 *kg* in weight. The propulsion system of this vehicle consists of six thrusters to obtain a fully actuated system.

The underwater robot is driven by a laptop computer, with CPU Intel Core i7-3520M 2.9 GHz, 8GB of RAM. The computer runs under Windows

7 operating system, and the control software is developed with Visual C++ 2010. The computer receives the data from the ROV's sensors (pressure, IMU), computes the control laws and sends input signals to the actuators. Syren 25 Motor Drives control these latter. The main features of this vehicle are described in Table 1. The control algorithm was experimentally tested in

Mass	28 kg
Buoyancy	9 N
Dimensions	75×45 cm
Maximal depth	100m
Thrusters	6 Seabotix BTD150
Power	48V - 600 W
Attitude Sensor	Sparkfun Arduimu V3
	Invensense MPU-6000 MEMS 3-axis gyro and accelerometer
	3-axis I2C magnetometer HMC-5883L
	Atmega328 microprocessor
Camera	Pacific Co. VPC-895A
	CCD1/3 PAL-25-fps
Depth sensor	Preassure Sensor Breakout-MS5803-14BA
Sampling period	40 ms
Surface computer	
Dell Latitude E6230- Intel Core i7 -2.9 GHz	
	Windows 7 Professional 64 bits
	Microsoft Visual C++ 2010
Tether length	150 m

Table 1: Main Features of the underwater vehicle

the $4 \times 4 \times 1.2$ m pool of the LIRMM (see Fig. 11). Although the proposed control law was given by (10) is designed for the whole system of six degrees of freedom, the real-time experiments shown in this article concern only depth and yaw motions. The primary objective of the designed control law is to robustly track a desired trajectory in depth and yaw despite parameter uncertainties and external disturbances.

4.1. Proposed Scenarios and Technical Details

To test the robustness of the proposed controller, four different scenarios have been performed, namely:

1. Scenario 1: Nominal case.
   In this scenario, the AUV follows the desired trajectory in depth and yaw simultaneously in the absence of external disturbances or parametric uncertainties. During this test, the controller's gains are adjusted to obtain the best tracking performance. These gains remain unchanged during all the remaining experiments.
2. Scenario 2: Robustness towards parametric uncertainties.
   In this test, the buoyancy and damping of the vehicle were modified to test the effectiveness of the controller and its robustness towards parametric uncertainties.
3. Scenario 3: Robustness towards external disturbances.
   This test was inspired by a more realistic scenario, where the vehicle has the task of loading an object and when reaching a certain depth, dropping that object. In this test, it is possible to observe a sudden change in the vehicle's weight and how it affects the controller performance.
4. Scenario 4: Robustness towards disturbances in the control law.
   In this experiment, the controller was perturbed though an aggressive disturbance generated by software to show the advantages of the adaptive algorithm towards persistent disturbances.

During the listed experiments, the adaptive controller was compared against the GSTA nominal design with constant gains to show the improvements of the proposed controller. The GSTA was tuned heuristically but always considering the constraints given by the stability proofs shown in [28]. For example, the GSTA could be seen as a kind of nonlinear PI controller and the tuning procedure is enclosed as follows:

1. Fix the values $\mu_{1i} = \mu_{2i} = 1$, $\Lambda_i = 1$ and $k_{23} = 0.0001$ and the gain k_{1i} is increased until the controller reaches the desired value and starts to oscillate.
2. Decrease a fraction of k_{1i} and then increase the value of k_{23} slightly until the oscillation in steady state decrease.
3. The rate of convergence to the desired signal is modified through the value of Λ_i.

In order to prevent the chattering effect in the GSTA control input, it is suggested to keep the gain k_{2i} in a small value. After tuning the algorithm for a constant reference, the control law was tested for a trajectory tracking task without considering external disturbances (nominal case), where the values of the gains were improved until reach a good performance and can be seen in Table 2.

The tuning process of the adaptive controller is summarized in the following steps:

1. Using the values of μ_{1i}, μ_{2i} and Λ_i found in the previous case, fix the values $\varsigma_i = 1$ and $\omega_i = 0.01$. To modify the convergence velocity to the set-point, the parameter ω_i need to be increased.
2. Fix the parameters $\epsilon_i = 0.01$ and $\beta_i = 0.01$. Then, slightly increase the value of one of the two mentioned parameters until oscillations in steady-state decrease.

The chosen parameters are shown in Table 3.

Finally, it is necessary to emphasize that the gains of the adaptive controller shown in equation (12) depend directly over the sliding surface $\sigma(t)$. Moreover, $\sigma(t)$ is related to the underwater vehicle system state η as stated in (9). In practice, sensors which provide the data η, supply noisy measurements. Thus, the condition $\sigma(t) = 0$ is not realistic and never satisfied which leads to a steady growth of the controller gains $k_1(t)$ and $k_2(t)$. To overcome the mentioned drawback, the condition (12) is modified as follows:

$$\dot{k}_{1i}(t) = \begin{cases} 0 & \text{if } -\varepsilon_i \leq \sigma \geq \varepsilon_i \\ \mu_{1i}\sqrt{\frac{\varsigma_{1i}}{2}} & \text{otherwise} \end{cases} \tag{43}$$

$$k_{2i}(t) = 2\epsilon_i k_{1i}(t) + \beta_i + 4\epsilon_i^2 \tag{44}$$

where ε is a small positive parameter.

Depth	$k_{13} = 0.30$	$k_{23} = 0.005$	$\Lambda_3 = 2.5$
Yaw	$k_{16} = 2.0$	$k_{26} = 0.15$	$\Lambda_6 = 6.0$

Table 2: GSTA controller gains used in real-time experiments

4.2. Control in nominal conditions

The upper plot of Figure 2 shows the depth and yaw tracking controller performance of the robot during the first case. In this experiment, the vehicle follows a trajectory in depth going from the surface to a maximal depth of 30 cm, where the vehicle remains stable in that position for 20 seconds and

Depth	$\mu_3 = 0.1$	$\varsigma_3 = 1.0$	$\Lambda_3 = 2.5$
	$\epsilon_3 = 0.01$	$\beta_3 = 0.035$	$\varepsilon_3 = 0.1$
Yaw	$\mu_6 = 0.3$	$\varsigma_6 = 1.0$	$\Lambda_6 = 6.0$
	$\epsilon_6 = 0.01$	$\beta_6 = 0.10$	$\varepsilon_6 = 0.1$

Table 3: Adaptive control gains used in real-time experiments

	Adaptive		GSTA	
	$RMSE_z$ $[m]$	$RMSE_\psi$ $[deg]$	$RMSE_z$ $[m]$	$RMSE_\psi$ $[deg]$
Scenario	Depth	Yaw	Depth	Yaw
1	0.0013	0.2077	0.0027	0.2872
2	0.0196	0.1758	0.0897	0.6375
3	0.0200	0.1147	0.0648	0.3063
4	0.0101	1.2541	0.0713	2.6987

Table 4: Control gains used in real-time experiments

finally emerges to 20 cm and hovers until the trial ends. For the yaw motion, the vehicle turns from its initial position to 60 degrees in 6 seconds. Then, it remains stable in that position for 20 seconds. Finally, the robot goes to -60 degrees and stay there until the test ends. It can be noticed that the GSTA controller takes a short lapse of time to converge to the reference while the adaptive version takes about 15 seconds to converge to the reference signal. This behavior can be explained because the gains of the adaptive controller are selected by a dynamic equation which is updating itself depending on the sliding surface σ value. When the value of σ is far from zero, the gains of the adaptive algorithm is increased until the condition (30) is reached. Besides, the tracking error evolution is shown in the middle of Figure 2 and can be analyzed through numerical data of Root Mean Square Error (RMSE) which is displayed in Table 4. The numerical results of Table 4 show an improvement of the adaptive controller over the nominal design. Also, the behavior of the control inputs is displayed at the bottom of Figure 2. From this Figure, it can be noticed that the control signal of the adaptive controller is smoother than the control signal of the nominal GSTA. Finally, the evolution of the adaptive controller gains is shown in Figure 3.

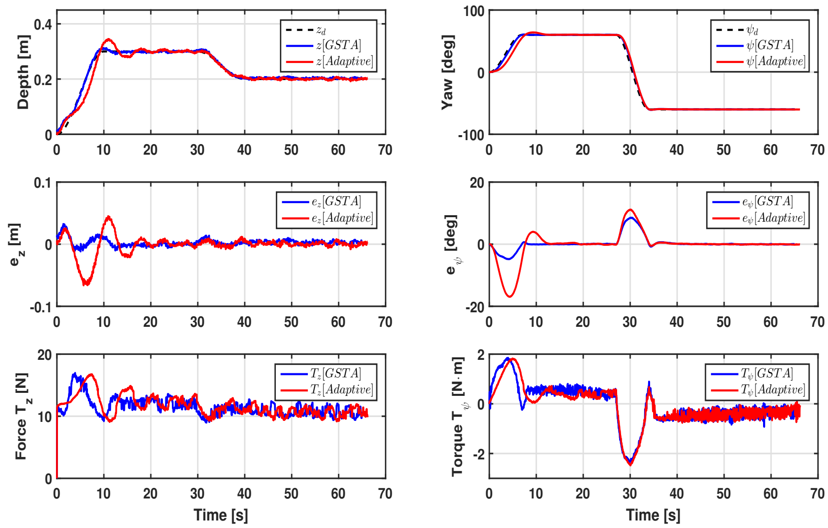

Figure 2: Performance comparison of the GSTA (blue line) and the adaptive GSTA (red line). (Upper) Trajectory tracking in depth and yaw in absence of disturbances. (Middle) Plots of the error signal. (Lower) Evolution of the control inputs.

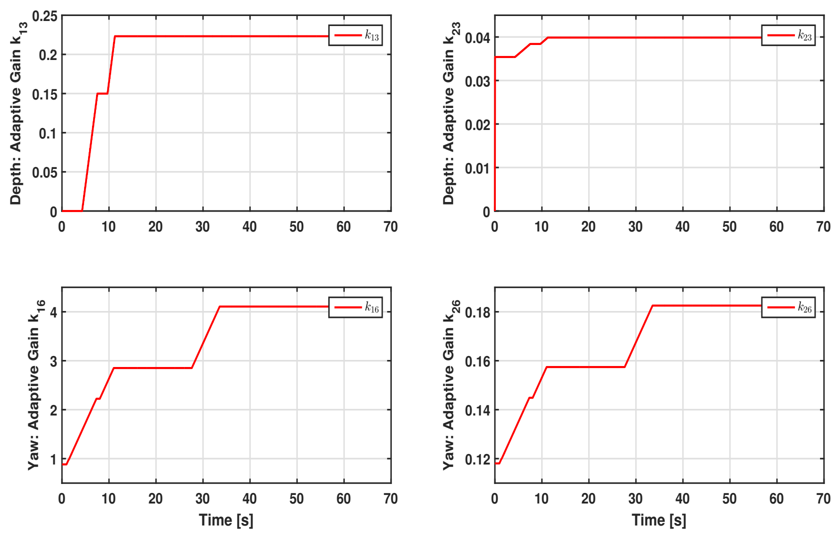

Figure 3: Evolution of the adaptive controller gains. (Upper) Updating of the gains for depth trajectory tracking. (Lower) Evolution of the gains for the yaw trajectory tracking test.

4.3. Control towards parametric uncertainties

To evaluate the robustness of the proposed controller against parametric uncertainties, the buoyancy of the vehicle was modified by tying two floats to the sides of the robot, increasing the floatability by 200%. To modify the damping of the submarine, a large rigid sheet of plastic that has a dimension of 45×10 cm was attached on one side of the vehicle, increasing the rotational damping along the z-axis by approximately 90%.

The trajectory tracking for depth and yaw motion is shown in the top of Figure 4. On the one hand, due to the large persistent disturbance in heave motion, the nominal GSTA controller is not capable of following the depth reference signal. On the other hand, the adaptive GSTA only takes about 15 seconds to converge to the reference depth trajectory despite the parametric disturbance in heave motion. Furthermore, the behavior of both controllers is similar during the yaw trajectory tracking test. The plot of the tracking errors is displayed in the middle of Figure 4. It should be noted the fast convergence of the adaptive algorithm over the nominal design performance. As mentioned before, the tracking in yaw is similar for both cases. The RMSE for the controller's couple is summarized in Table 4. As in the nominal case, the improvement of the adaptive version over the nominal GSTA is demonstrated through numerical data. Also, in the bottom of Figure 4 we can observe the progress of the control inputs. For example, for the depth following, we can observe that the force increases almost twice compared with the nominal case, this suggests that there is a strong compromise between the controller's ability to reject disturbances with the increase in energy that is demanded from the actuators. Finally, the evolution of the adaptive gains of the GSTA is shown in Figure 5. It is important to note that the gains update itself every time that the robot submerges, emerges or turns.

4.4. Control towards external disturbances

In some applications, underwater vehicles are equipped with robotic manipulators which allow to carry objects and take them to a specific depth or pick them up from the ocean floor to transport them to the surface. That practical case inspires this scenario, to simulate that the robot carries a load, a metallic block of 1 kg was tied to the submarine with a rope of a length about 20 cm. In this scenario, the maximal depth of the reference trajectory was set at 40 cm. Regarding the maximum depth of the basin is 50 cm, the robot will be suddenly disturbed when it reaches 30 centimeters, because the metallic block will touch the floor, thus suddenly canceling its weight's effect.

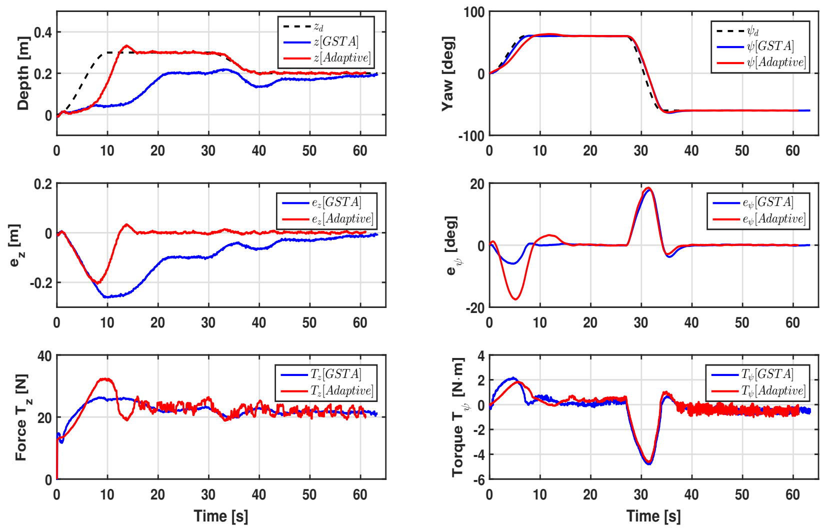

Figure 4: Robustness of the GSTA (blue line) and the Adaptive GSTA (red line) controller performance towards parametric uncertainties. The floatability of the submarine was increased 200% while the damping along z-axis was modify up to 90% respect the nominal case.

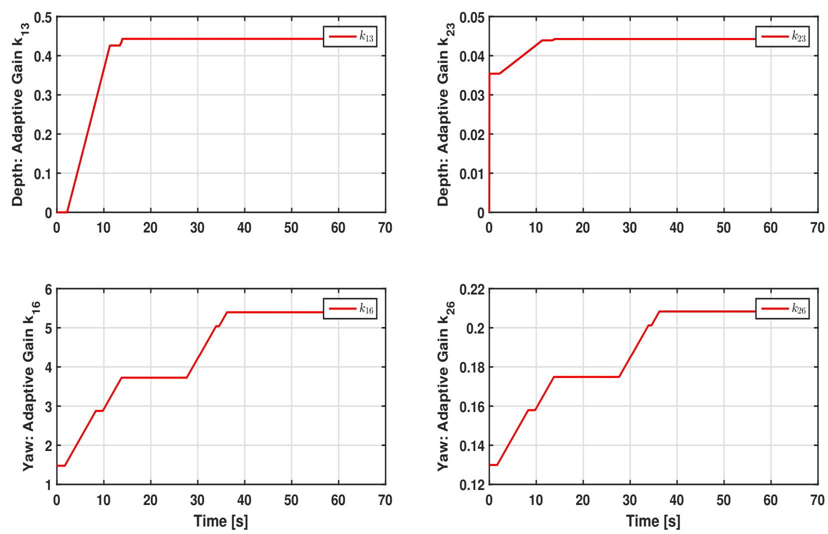

Figure 5: Evolution of the adaptive controller gains. (Upper) Updating of the gains for depth trajectory tracking. (Lower) Evolution of the gains for the yaw trajectory tracking test.

The disturbance will be acting on the robot until it starts to emerge and it reaches 30 cm, the action of the extra weight will influence the trajectory of the submarine again (see Figure 6).

The results of the controller's performance in the robustness test against external disturbances are shown in Figure 7. At the top of the graph, the initial position of the vehicle is at 30 cm deep due to the influence of the added extra weight. When the test begins, the robot reaches the desired trajectory in about 5 and 15 seconds under the nominal GSTA and the adaptive controller, respectively. In the 10th second, the 1kg block touches the floor, and the total weight of the vehicle suddenly changes. Both controllers are capable of compensating the effect of the disturbance some seconds later. When the vehicle emerges, the extra weight acts again on the submarine degrading the trajectory tracking. While the nominal GSTA cannot compensate the disturbance's effect, the adaptive algorithm counteracts the perturbation impact, and the submarine converges to the reference signal accurately. The error plots are displayed at the middle of Figure 7, while the numerical value of the RMSE is shown in Table 4. The control input signals are shown at the bottom of Figure 7. Finally, the evolution of the adaptive controller gains is shown in Figure 8.

4.5. Control signal disturbed by software

Most of the commercial underwater vehicles have two maneuvering modes: ROV and Autonomous mode. When the vehicle is performing a task autonomously, and a mechanical failure or a wrong behavior occurs, the vehicle's operator can switch from one mode to another in order to prevent damage to the environment or the vehicle itself. Switching from one mode to another can take a few seconds if the vehicle is performing a mission at considerable depth and suddenly an actuator's drives fail,then, a few seconds could represent a big issue because the operator can lose the robot. Based on the mentioned scenario, while the underwater vehicle is performing the trajectory tracking as in the same conditions as in the nominal case, a constant signal (see Figure X) is introduced to the robot control input to simulate a failure in the actuator's driver.

The tracking trajectory for depth and yaw is shown in the upper part of Figure 9. From the tracking in depth, it can be noted that both controllers have the same rate of convergence as in the nominal case. However, the performance of the nominal GSTA is highly degraded when the simulated failure on the robot actuator appears while the Adaptive controller can compensate

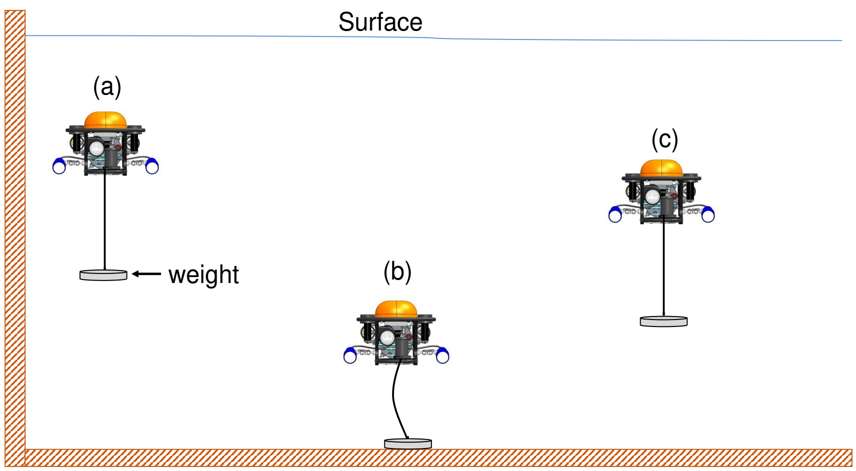

Figure 6: Description of the robustness towards external disturbances test. (a) 1 kg weight is attached to the submarine, (b) the action of the extra weight disappears when the vehicle reaches 30 cm in depth. Again, the robot is disturbed by the weight when the vehicle emerges (c).

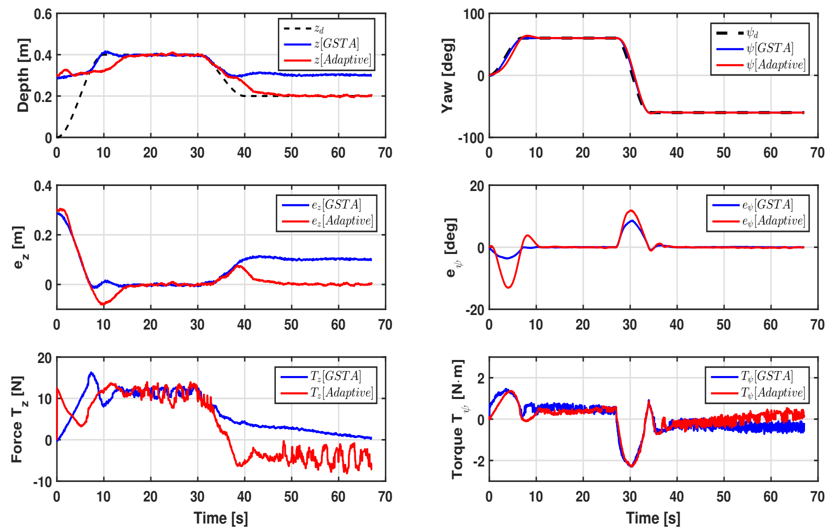

Figure 7: Performance of the proposed controller towards external disturbances test. (Upper) Trajectory tracking in depth and yaw: The 1 kg block is attached to the submarine which produced disturbances at 8 and 35 seconds when the block touches and takes off the floor, respectively. (Middle) Plots of the error signal. (Lower) Evolution of the control inputs.

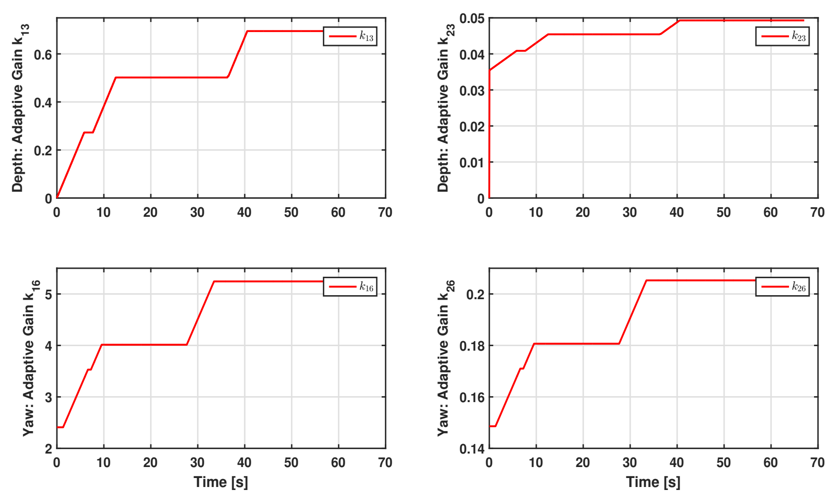

Figure 8: Evolution of the adaptive controller gains. (Upper) Updating of the gains for depth trajectory tracking. (Lower) Evolution of the gains for the yaw trajectory tracking test.

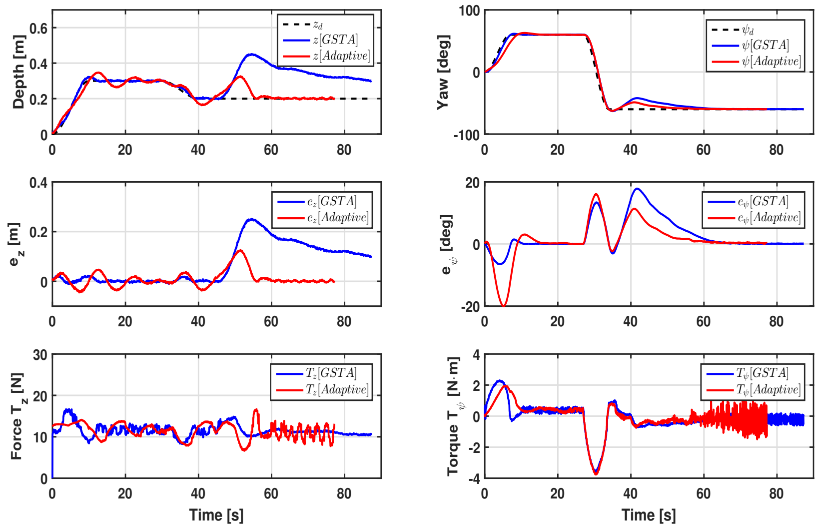

Figure 9: Underwater Vehicle actuators failure test: A large signal is introduced to the input signal acting as a disturbance at 45th second. (Upper) Trajectory tracking in depth and yaw of the GSTA (blue line) and the adaptive controller (red line). (Middle) Plots of the error signal. (Lower) Evolution of the control inputs.

the disturbance fast. On the other hand, the yaw tracking test shows again that the adaptive control performance is superior compared over the GSTA with constant gains.

In the middle of Figure 9, the plot of errors are depicted and the improvement of each controller is visually apparent and can be confirmed numerically through the RMSE Table 4. Also, the control inputs are displayed at the bottom of Figure 9. From this part of the Figure, it is worth to observe that there is a trade-off between the adaptive controller ability to reject large constant disturbances and the high controller gains. It means, based on the dynamic equation to select the controller gains, larges disturbances will be attenuated by high values of k_1 and k_2. Finally, the evolution of the adaptive controller gains is shown in Figure 10. Is interesting observe how the gains are increased when the disturbance is introduced into the control input.

5. Conclusions

In this paper, an decoupled adaptive high order sliding mode control has been developed for trajectory tracking control of an autonomous under-

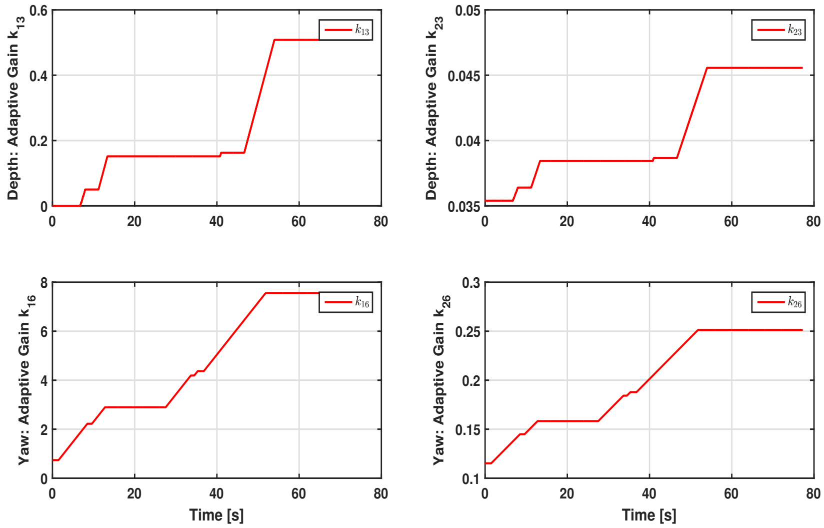

Figure 10: Evolution of the adaptive controller gains. Updating of the gains for depth trajectory tracking (Upper) and the yaw trajectory tracking control (Lower).

water vehicle. A Lyapunov design was proposed to prove the stability of the closed-loop system. The proposed controller has been implemented for trajectory tracking in depth and yaw motions on the LEONARD ROV underwater vehicle. The obtained real-time experimental results demonstrate the effectiveness and robustness of the proposed control law towards external disturbances and persistent parametric uncertainties.

Acknowledgment

This work was supported by Conacyt, grant 490978. The Leonard underwater vehicle has been financed by the European Union (FEDER grant n° 49793) and the Region Occitanie (ARPE Pilot Plus project).

[1] Y. C. Sun, C. C. Cheah, Adaptive control schemes for autonomous underwater vehicle, Robotica 27 (2009) 119–129.

[2] S. Zhao, J. Yuh, Experimental study on advanced underwater robot control, IEEE transactions on robotics 21 (2005) 695–703.

[3] D. A. Smallwood, L. L. Whitcomb, Model-based dynamic positioning of underwater robotic vehicles: theory and experiment, IEEE Journal of Oceanic Engineering 29 (2004) 169–186.

[4] T. I. Fossen, Guidance and control of ocean vehicles, John Wiley & Sons Inc, 1994.

[5] P. Herman, Decoupled pd set-point controller for underwater vehicles, Ocean Engineering 36 (2009) 529–534.

[6] X. Xiang, C. Yu, L. Lapierre, J. Zhang, Q. Zhang, Survey on fuzzy-logic-based guidance and control of marine surface vehicles and underwater vehicles, International Journal of Fuzzy Systems 20 (2018) 572–586.

[7] M. H. Khodayari, S. Balochian, Modeling and control of autonomous underwater vehicle (auv) in heading and depth attitude via self-adaptive fuzzy pid controller, Journal of Marine Science and Technology 20 (2015) 559–578.

[8] R. Cui, C. Yang, Y. Li, S. Sharma, Adaptive neural network control of auvs with control input nonlinearities using reinforcement learning, IEEE Transactions on Systems, Man, and Cybernetics: Systems 47 (2017) 1019–1029.

[9] Z. Yan, M. Wang, J. Xu, Global adaptive neural network control of underactuated autonomous underwater vehicles with parametric modeling uncertainty, Asian Journal of Control (2019).

[10] C. Shen, Y. Shi, B. Buckham, Trajectory tracking control of an autonomous underwater vehicle using lyapunov-based model predictive control, IEEE Transactions on Industrial Electronics 65 (2018) 5796–5805.

[11] J.-H. Li, P.-M. Lee, Design of an adaptive nonlinear controller for depth control of an autonomous underwater vehicle, Ocean engineering 32 (2005) 2165–2181.

[12] L. G. García-Valdovinos, T. Salgado-Jiménez, M. Bandala-Sánchez, L. Nava-Balanzar, R. Hernández-Alvarado, J. A. Cruz-Ledesma, Modelling, design and robust control of a remotely operated underwater vehicle, International Journal of Advanced Robotic Systems 11 (2014) 1.

[13] H. Joe, M. Kim, S.-c. Yu, Second-order sliding-mode controller for autonomous underwater vehicle in the presence of unknown disturbances, Nonlinear Dynamics 78 (2014) 183–196.

[14] Z. H. Ismail, V. W. Putranti, Second order sliding mode control scheme for an autonomous underwater vehicle with dynamic region concept, Mathematical Problems in Engineering 2015 (2015).

[15] I. D. Landau, R. Lozano, M. M'Saad, A. Karimi, Adaptive control: algorithms, analysis and applications, Springer Science & Business Media, 2011.

[16] Y. Shtessel, C. Edwards, L. Fridman, A. Levant, Sliding mode control and observation, volume 10, Springer, 2014.

[17] T. Gonzalez, J. A. Moreno, L. Fridman, Variable gain super-twisting sliding mode control, IEEE Transactions on Automatic Control 57 (2012) 2100–2105.

[18] Y. Shtessel, M. Taleb, F. Plestan, A novel adaptive-gain supertwisting sliding mode controller: Methodology and application, Automatica 48 (2012) 759–769.

[19] N. Q. Hoang, E. Kreuzer, A robust adaptive sliding mode controller for remotely operated vehicles, Technische Mechanik 28 (2008) 185–193.

[20] R. Cui, X. Zhang, D. Cui, Adaptive sliding-mode attitude control for autonomous underwater vehicles with input nonlinearities, Ocean Engineering 123 (2016) 45–54.

[21] Z. Chu, D. Zhu, S. X. Yang, G. E. Jan, Adaptive sliding mode control for depth trajectory tracking of remotely operated vehicle with thruster nonlinearity, The Journal of Navigation 70 (2017) 149–164.

[22] G.-c. Zhang, H. Huang, L. Wan, Y.-m. Li, J. Cao, Y.-m. Su, et al., A novel adaptive second order sliding mode path following control for a portable auv, Ocean Engineering 151 (2018) 82–92.

[23] Y. Wang, L. Gu, M. Gao, K. Zhu, Multivariable output feedback adaptive terminal sliding mode control for underwater vehicles, Asian Journal of Control 18 (2016) 247–265.

[24] L. Qiao, W. Zhang, Adaptive second-order fast nonsingular terminal sliding mode tracking control for fully actuated autonomous underwater vehicles, IEEE Journal of Oceanic Engineering (2018).

[25] M. Sarfraz, F. u. Rehman, I. Shah, Robust stabilizing control of nonholonomic systems with uncertainties via adaptive integral sliding mode: An underwater vehicle example, International Journal of Advanced Robotic Systems 14 (2017) 1729881417732693.

[26] A. Levant, Sliding order and sliding accuracy in sliding mode control, International journal of control 58 (1993) 1247–1263.

[27] Y. B. Shtessel, J. A. Moreno, F. Plestan, L. M. Fridman, A. S. Poznyak, Super-twisting adaptive sliding mode control: A lyapunov design, in: Decision and Control (CDC), 2010 49th IEEE Conference on, IEEE, pp. 5109–5113.

[28] J. A. Moreno, A linear framework for the robust stability analysis of a generalized super-twisting algorithm, in: Electrical Engineering, Computing Science and Automatic Control, CCE, 2009 6th International Conference on, IEEE, pp. 1–6.

[29] K. D. Do, J. Pan, Control of ships and underwater vehicles: design for underactuated and nonlinear marine systems, Springer Science & Business Media, 2009.

[30] G. Antonelli, T. I. Fossen, D. R. Yoerger, Underwater robotics, in: Springer handbook of robotics, Springer, 2008, pp. 987–1008.

[31] T. T. J. Prestero, Verification of a six-degree of freedom simulation model for the REMUS autonomous underwater vehicle, Ph.D. thesis, Massachusetts institute of technology, 2001.

[32] J. Vervoort, Modeling and control of an unmanned underwater vehicle, Ph.D. thesis, Ph. D. thesis, University of Canterbury, 2009.

[33] S. of Naval Architects, M. E. U. Technical, R. C. H. Subcommittee, Nomenclature for Treating the Motion of a Submerged Body Through a Fluid: Report of the American Towing Tank Conference, Technical and research bulletin, Society of Naval Architects and Marine Engineers, 1950.